



LAWRENCE  
LIVERMORE  
NATIONAL  
LABORATORY

# Modeling the material properties at the onset of damage initiation in bulk potassium dihydrogen phosphate crystals

S. G. Demos, M. D. Feit, G. Duchateau

October 22, 2014

SPIE Laser Damage Conference 2014  
Boulder, CO, United States  
September 14, 2014 through September 17, 2014

## **Disclaimer**

---

This document was prepared as an account of work sponsored by an agency of the United States government. Neither the United States government nor Lawrence Livermore National Security, LLC, nor any of their employees makes any warranty, expressed or implied, or assumes any legal liability or responsibility for the accuracy, completeness, or usefulness of any information, apparatus, product, or process disclosed, or represents that its use would not infringe privately owned rights. Reference herein to any specific commercial product, process, or service by trade name, trademark, manufacturer, or otherwise does not necessarily constitute or imply its endorsement, recommendation, or favoring by the United States government or Lawrence Livermore National Security, LLC. The views and opinions of authors expressed herein do not necessarily state or reflect those of the United States government or Lawrence Livermore National Security, LLC, and shall not be used for advertising or product endorsement purposes.

# Modeling the material properties at the onset of damage initiation in bulk potassium dihydrogen phosphate crystals

Stavros G. Demos<sup>1</sup>, Michael D. Feit<sup>1</sup>, Guillaume Duchateau<sup>2</sup>

<sup>1</sup> Lawrence Livermore National Laboratory, 7000 East Ave., Livermore, CA 94551, USA

<sup>2</sup> Université de Bordeaux-CNRS-CEA, Centre Lasers Intenses et Applications, UMR5107, 351 Cours de la Libération, 33405 Talence, France

## ABSTRACT

A model simulating transient optical properties during laser damage in the bulk of KDP/DKDP crystals is presented. The model was developed and tested using as a benchmark its ability to reproduce the well-documented damage initiation behaviors but most importantly, the salient behavior of the wavelength dependence of the damage threshold. The model involves two phases. During phase I, the model assumes a moderate localized initial absorption that is strongly enhanced during the laser pulse via excited state absorption and thermally driven generation of additional point defects in the surrounding material. The model suggests that during a fraction of the pulse duration, the host material around the defect cluster is transformed into a strong absorber that leads to significant increase of the local temperature. During phase II, the model suggests that the excitation pathway consists mainly of one photon absorption events within a quasi-continuum of short-lived vibronic defect states spanning the band gap that was generated after the initial localized heating of the material due to thermal quenching of the excited state lifetimes. The width of the transition (steps) between different number of photons is governed by the instantaneous temperature, which was estimated using the experimental data. The model also suggests that the critical physical parameter prior to initiation of breakdown is the conduction band electron density. This model, employing very few free parameters, for the first time is able to quantitatively reproduce the wavelength dependence of the damage initiation threshold, and thus provides important insight into the physical processes involved.

**Keywords:** KDP, DKDP, laser-induced damage, theoretical modeling laser damage.

## 1. INTRODUCTION

A key feature of laser-induced damage is that it transforms a nominally transparent non-absorbing material into a plasma with temperatures on the order of 1 eV and pressures on the order of 10 GPa [1-4]. This transformation occurs while the physical properties of the material are rapidly modified while hydrodynamic expansion effects can play an important role. The origin of damage has been extensively explored for more than 50 years and a general understanding of the processes involved has been developed. More than 40 years ago, Anisimov *et al* [5] concluded that “*If the light intensity exceeds a certain critical value, a wave of heating and light absorption arises and propagates in to the medium. The effective size of the absorbing region increases...*” and “*...the absorption coefficient be a strong function of the temperature.*” The same year, N. Bloembergen [6] argued that “*The concentration of the electric field strength in the neighborhood of micropores and cracks may lower the nominal external intensity for electric avalanche breakdown by a factor 2-100...*” and “*...the presence of absorbing inclusions at edge of microcracks will be the dominant mechanism*”. In spite of significant progress in producing higher damage resistance optical materials, the description of how the nominally transparent material is transformed to a strong absorber remains qualitative and existing models are limited.

KDP (and DKDP) crystals are suitable candidate material for modeling the transient material properties at the onset of damage initiation because: (a) KDP exhibits a low melting point (on the order of 400 K), so phase transition and damage related processes take place at a lower temperature with limited influence of hydrodynamic effects; (b) there is significant prior work documenting their damage initiation behaviors as well as experimental results that probed the electronic structure of the damage precursors. Specifically, there are a number of studies that have measured a number of key aspects of the laser induced damage behavior of bulk KDP/DKDP crystals including a) the wavelength [7] and pulse length [8] dependence of the damage threshold as well as under exposure to multiple wavelengths [9-12]. These results

\*Corresponding author: demos1@llnl.gov

provide indirect information about the underlying processes that govern the dynamics of the energy deposition process. In turn, these processes are related to the transient material optical properties that enable the coupling of the laser energy to the material. A number of models have been proposed that typically involve the presence of damage precursors that couple energy into the material via linear absorption. However, although such models were able to reproduce a subset of the damage behaviors under specific excitation conditions, they contain no physical mechanisms that can anticipate the observed wavelength dependence of the laser-induced damage threshold (LIDT). It was proposed that damage may involve a multistep absorption mechanism but no specific physical scenario and associated modeling were suggested [7].

The goal of this work is to develop such a model to describe the transient optical properties in KDP/DKDP crystals at the onset of bulk damage initiation. We test the model by using as a benchmark its ability to reproduce well-documented damage initiation behaviors. This allows us to estimate the value of some of the physical parameters involved and provides insight into the processes involved during damage initiation leading to plasma formation. As the final stage of the process involves the formation of warm dense matter (with solid density and temperature in the eV range), this model also helps to enhance the understanding of the physical processes in a regime that remains largely unexplored.

## 2. RESULTS

This effort is motivated by experimental results that have been described elsewhere. In particular, there are two key spectroscopic damage-testing results that have revealed salient behaviors of the damage threshold as a function of the laser wavelength that provide the basis for the development of this model. These key results are shown in Figure 1. Specifically, Figure 1a shows the LIDT in DKDP as a function of the laser wavelength. A detailed description of the experiments is provided in Ref 7. These results demonstrate that the damage threshold exhibits steps at photon energies that correspond to submultiples of the material bandgap. This in turn suggests the direct involvement of the host material rather than a “foreign” precursor (such as impurities or stoichiometric defects). However, the size of the “steps” is very small compared to that expected for typical nonlinear mechanisms such as multiphoton absorption. Figure 1b shows the relative damage efficiency ( $\gamma$ ) of  $2\omega$  pulses compared to  $3\omega$  pulses as a function of the individual and combined exposure fluence at these wavelengths. A detailed description of the experiments is provided in Ref. 12. The damage efficiency is defined as the ratio of the  $3\omega$  fluence that can replace certain  $2\omega$  fluence under simultaneous exposure to  $2\omega$  and  $3\omega$  laser pulses to generate the same measured damage density. In simple terms, what  $3\omega$  laser fluence is needed (nominator) to replace certain  $2\omega$  laser fluence (denominator) to cause the same amount of damage. For example, assuming a linear absorption model, the relative damage efficiency should be a constant. Instead, the results shown in Figure 1b indicate the  $\gamma$  varies widely, depending on the individual fluence at each wavelength. For higher fluences the value is about 0.8 but for lower fluences this value can be as low as roughly 0.2. Interestingly, the value of  $\gamma$  starts at about 0.4 at the lowest fluences but then decreases to roughly 0.2 before it recovers. This suggests a “bottleneck” in the excitation pathway that makes the  $2\omega$  light less efficient in generating damage as the laser intensity increases.

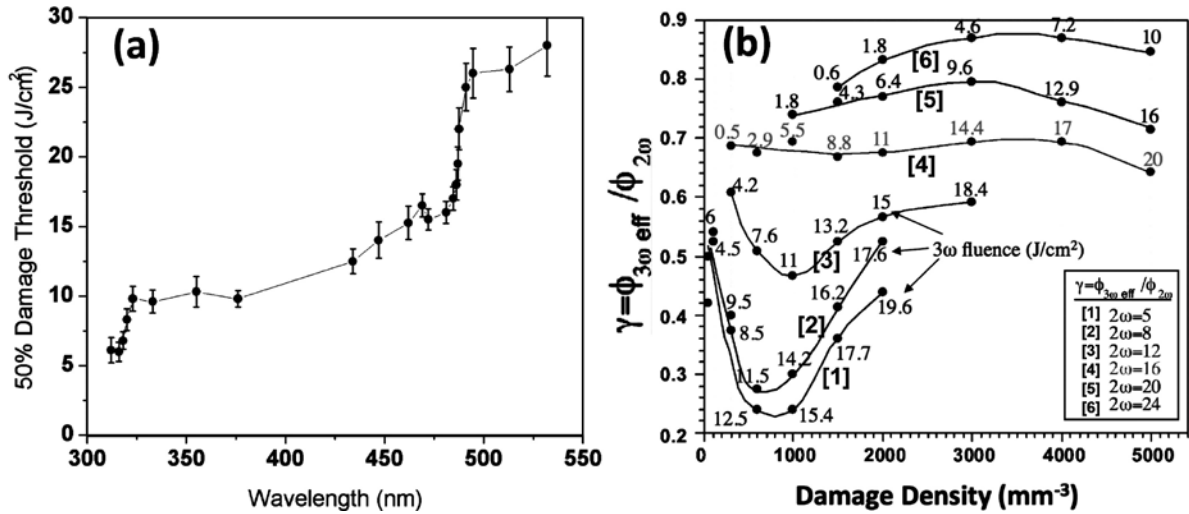


Figure 1. Spectroscopic damage testing in bulk DKDP material. a) The laser induced damage threshold vs wavelength. b) The relative Damage Efficiency at  $2\omega$  and  $3\omega$ .

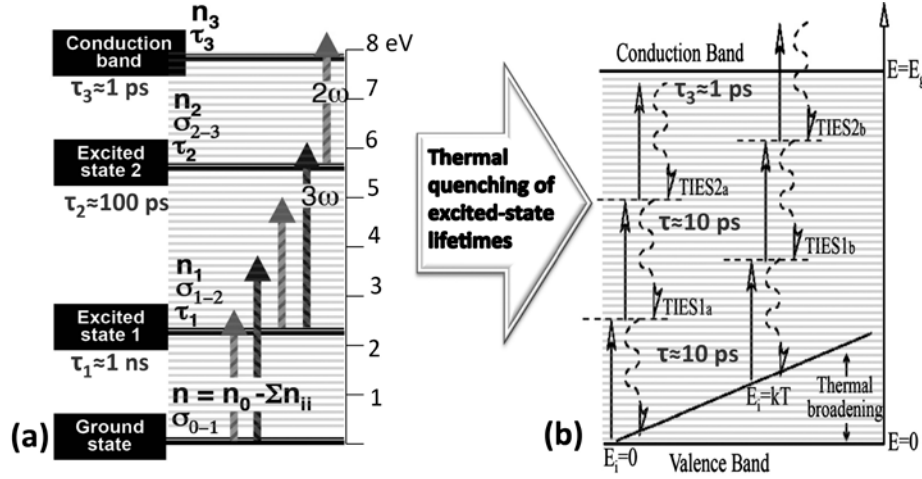


Figure 2. Schematic depiction of the electronic structure and excitation pathway of the defect clusters in bulk KDP/DKDP crystals a) before and b) after thermal quenching of the excited state lifetimes.

Assuming that damage initiates for the energy deposition to a precursor, the decrease of  $\gamma$  with increasing excitation conditions may be attributed to the electronic structure of the precursor (light absorbing) defect. Thus, we proposed that nanometric defects incorporated in the crystal lattice induce electronic states in the band gap that can facilitate excitation of valence electrons into the conduction band through sequential one-photon absorption events, thus, *a priori* providing the mechanism for energy deposition and heating in the course of the interaction with the laser pulse. In addition, the electronic structure contains a series of excited states with the energy separation between the 1<sup>st</sup> to the 2<sup>nd</sup> excited state able to be bridged through a single photon absorption at  $3\omega$  but not at  $2\omega$ . We postulated that this difference in the energy separation (between the 1<sup>st</sup> to the 2<sup>nd</sup> states) produces the mechanism that supports the observed “bottleneck”. A schematic depiction of the projected electronic structure is shown in Figure 2a.

Based on this structure, a rate equation system to describe the transition of electrons from the ground state to the conduction band was developed. This approach was described in detail in Ref. 12. Assuming that the generated energy from non-radiative relaxation leads to temperature rise (while not including additional effects discussed later, which do not affect the model generated behavior of  $\gamma$ ), this general approach reproduces the general behavior of the relative damage efficiency ( $\gamma$ ) shown in Figure 1b. This model also reproduced the measured damage threshold values at  $3\omega$  as a function of laser pulse-length [8], further highlighting the potential of this approach to describe the damage initiation process. This approach assumed that damage initiation is associated with a “damage threshold temperature” where damage is initiated when the material reaches this threshold temperature. However, it must be recognized that the temperature and conduction band electron population are monotonically related within the description of this model, which implies that a “threshold temperature” is equivalent to a “threshold conduction band electron population”.

Based on these initial encouraging results, the rate equation system was expanded to include the concept that the energy deposited (local temperature rise) lead to generation of new defects through heat transfer. We assumed that these new defects cause additional absorption (within the damage precursor region and in the surrounding region), thus also satisfying the requirement that “the absorption coefficient be a strong function of the temperature” [5]. Time-resolved imaging results of laser induced damage initiation in bulk DKDP were also supportive of this hypothesis as described in more detail in Ref. 13. This hypothesis is also consistent with earlier work using nanoparticles as damage precursors [14]. This enabled us to model the evolution of the temperature, electronic densities, and absorbed power density as a function of time inside the expanding absorbing region as well as the dynamics of this expansion (driven purely by heat conduction and secondary defect generation). A detailed description of this work is presented in Ref. 13 for the case of damage initiation with  $3\omega$  pulses. Representative results from this effort are shown in Figure 3. Specifically, Figure 3a shows the evolution of the temperature at the center of the absorbing region as a function of time assuming flat in time laser pulses. The results show that about 300 ps from the onset of the laser pulse, a “thermal explosion” is taking place with the temperature of the material rapidly reaching over 1000 K, at about 600 ps. Figure 3b describes the absorbed laser energy by the electrons populating each of the excited states. The latter results show that at the time of “thermal

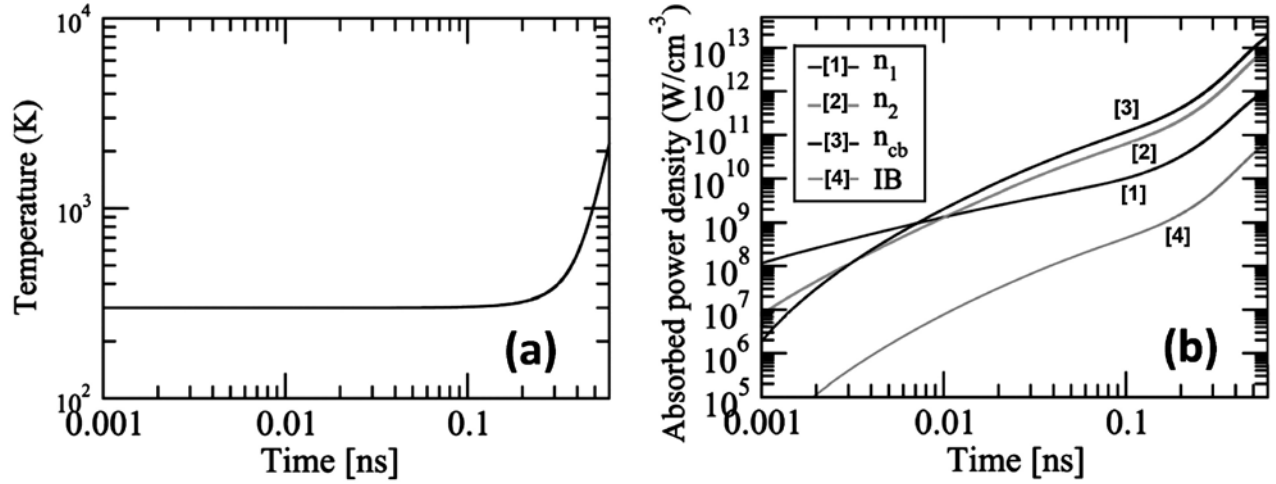


Figure 3. Model estimates of the dynamics of physical properties and energy balance. a) The temperature at the center of absorbing region. b) The absorbed power density from the electron population located in each state.

explosion”, the larger contribution arises from the electrons in the conduction band, followed by the electrons occupying the 2<sup>nd</sup> excited state. These results also yielded a number of fitting parameters, which were developed to fit the array of experimentally measured profiles shown in Figure 1b. Overall, the fitting and material parameters used in this model are summarized in table 1.

Table 1: Material parameters used in the modeling along with fitting parameters obtained from reproducing using the model the experimental observations

| Description of variables and parameters     | Symbol        | Value                                 |
|---------------------------------------------|---------------|---------------------------------------|
| Photon energy                               | $\hbar\omega$ | 3.54 eV                               |
| Laser intensity                             | $I$           | 3 GW/cm <sup>2</sup>                  |
| one-photon absorption cross section         | $\sigma_1$    | $1.5 \times 10^{-18}$ cm <sup>2</sup> |
| one-photon absorption cross section         | $\sigma'_1$   | $7\sigma_1$                           |
| Recombination time                          | $\tau_1$      | 1 ns                                  |
| Recombination time                          | $\tau_2$      | 50 ps                                 |
| Recombination time                          | $\tau_3$      | 1 ps                                  |
| Energy gap between ground state and level 1 | $E_{01}$      | 2.3                                   |
| Energy gap between level 1 and level 2      | $E_{12}$      | 3.2                                   |
| Energy gap between level 2 and CB           | $E_{23}$      | 2.2                                   |
| Collisional frequency                       | $\nu_c$       | $10^{15}$ s <sup>-1</sup>             |
| Heat capacity                               | $C$           | 2 J/K/cm <sup>3</sup>                 |
| Thermal diffusivity of DKDP                 | $D_i$         | $10^{-6}$ m <sup>2</sup> /s           |
| Room temperature                            | $T_0$         | 300 K                                 |
| Initial point defect density                | $n_0$         | $5 \times 10^{19}$ cm <sup>-3</sup>   |
| Maximum point defect density                | $K_0$         | $10^{22}$ cm <sup>-3</sup>            |
| Energy of a hydrogen bond in KDP            | $E_a$         | 0.042 eV                              |
| Radius of the precursor defect              | $r_0$         | 100 nm                                |

The model described above was able to reproduce the experimental results shown in Figure 1b as well as the pulse-length dependence of the damage threshold but when tested, it was unsuccessful to reproduce the wavelength dependence of the damage threshold. It was apparent that a component of the physics involved was missing from this

model. The results of Figure 1a suggest that the LIDT “steps” are related to the host material band structure while the model assumed the electronic structure of the precursors. It was clear that the missing physics was centered around this critical point. It was also apparent that the missing component in our model was not significantly affecting the overall behavior at a single wavelength but it was becoming important when varying the wavelength. We postulated that this missing component must be at the end of the assumed physical scenario, namely after the initiation of the “thermal explosion”. To address this issue, we considered all of the possible material parameters that can be significantly altered by the increase of the temperature. For example, phase transition can cause loss of energy and change of the electronic structure of the defects, but this could not yield the transition from the defect-centric electronic structure to the host-centric electronic structure that could conceivably thereafter reproduce the LIDT “steps” that correspond to submultiples of the host material bandgap.

The other physical process related to the increase of the material temperature is commonly referred to as “thermal quenching of the excited state lifetime”. This originates from the energy required to thermally excite electrons located near the lowest vibrational states of the excited states to stimulate their nonradiative relaxation, thus quenching (reducing) their excited state lifetime. This behavior is typically abrupt occurring within a narrow range of temperature where the lifetime of the excited state can change by two orders of magnitude or more [15-18]. Assuming this process in our model, the lifetime of the excited states (see table 1) will be reduced to be on the order of 10 ps or less. This is typically the lifetime for phonon relaxation, thus the lifetime of the excited state vibronic levels. As background information, these vibronic levels are always present in the electronic manifold of defects located in solid state materials and represents the coupling of an electronic state with a number of vibrational states. The vibronic states give rise to the broadening of the absorption spectrum as well as that of the emission spectrum. However, the emission typically arises from the lowest vibronic levels of the excited states as the electron nonradiatively relax. Also, transiently populated vibronic states also give rise to emission but the strength of this emission is very weak due their short lifetime and it typically is referred to as “hot luminescence”. Therefore, assuming within this model that the lifetime of the lowest energy vibronic states of the excited states becomes approximately equal to that of the rest of the vibronic states, the electronic structure of the defect system depicted in Figure 2a is transformed into a continuum of vibronic states bridging the region between the valance and the conduction bands as schematically depicted in Figure 2b.

The rate equation system is thus modified to include the continuum of vibronic states having lifetimes on the order of 10 ps and the thermal population of vibronic states by valance band electrons. A detailed description of this approach is provided in Ref. 19. It must be noted that this representation of the system represents the phase II of the material behavior, which follows the heating of the material during phase I via the (previously discussed) defect driven energy deposition. In addition, due to the short lifetimes of the vibronic states involved ( $\sim 10$  ps), the rate equation system is converging very fast, in less than about 100 ps. Thus, this model is applicable only for about 100 ps after the quenching of the defect excited state lifetimes. On the other hand, the electronic structure during phase II is significantly simpler than the original electronic structure involving only the valance and conduction bands with a continuum of vibronic states, all having the same lifetimes. As a result, the number of free parameters is very limited.

We first attempted to model the behavior of this system assuming that the transition rates between all vibronic states is always the same, independent of the wavelength nor the transition step within the electronic-vibrational system manifold. This is essentially an attempt to model the system using only *one* free parameter. The goal of this approach was to test the general predicted trends, namely the formation of “steps” in the LIDT as a function of wavelength, qualitatively similar to those observed in Figure 1a. However, we needed to choose the physical parameter that is associated with the “damage threshold” event. A threshold temperature or conduction band (cb) electron density has often been used as determining parameter of the damage threshold. These two quantities are functionally equivalent (monotonically related) when considering only a single wavelength. Our initial efforts assuming a “damage threshold temperature” to reproduce the experimental results of LIDT as a function of laser wavelength were not satisfactory. Efforts assuming a “threshold conduction band electron density” yielded excellent fits to the data. To our surprise, this very simple approach yielded an excellent fit to the data of the damage threshold as a function of wavelength (shown in Figure 1a) as depicted in the fitting results shown in Figure 4 as a broken line. In fact, the only free parameter used here is the one-photon absorption cross sections  $\Sigma_{i \rightarrow j} = 0.88 \times 10^{-18} \text{ cm}^2$ . Just this single parameter produces an excellent fit except for the predicted value of the damage threshold above the higher energy step ( $\approx 3.9$  eV) where it predict a LIDT of  $3.5 \text{ J/cm}^2$  compared to  $\approx 6 \text{ J/cm}^2$  measured. This difference is diminished by making the physically expected assumption that transitions terminating in the conduction band should exhibit a much higher absorption cross section. By assuming this to be  $\Sigma_{j \rightarrow \text{cb}} = 0.33 \times 10^{-17} \text{ cm}^2$ , a fit that is qualitatively seamless is produced as shown by the solid line fit in Figure 4.

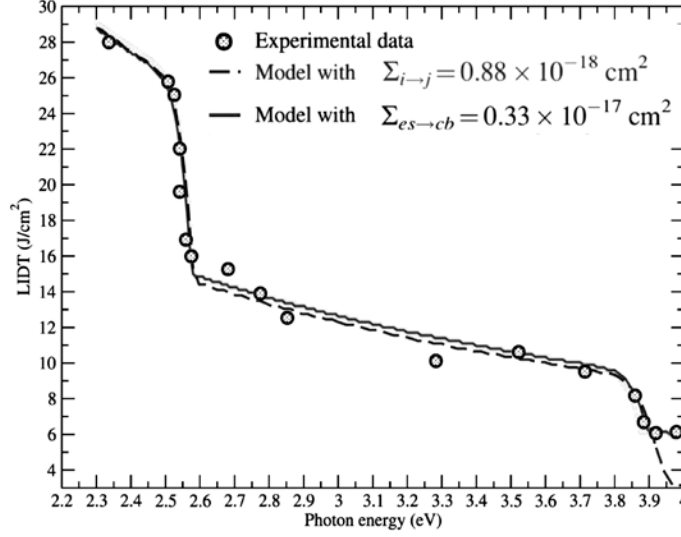


Figure 4. Model fit of the LIDT vs photon energy experimental results using a single value of the one-photon absorption cross sections for all transitions (broken line) and a different cross section for the transitions terminating in the conduction band (solid line).

A key feature of the LIDT vs wavelength experimental data is the width and contour of the step, especially that at 2.55 eV which is characterized by a larger number of experimental data points. Within our model, we found that the governing parameter of the profile of the LIDT step is the temperature. Higher assumed temperature leads to a larger width while smaller temperatures gives rise to a “steeper” step. This effect is demonstrated in Figure 5. We can therefore use the experimental results to estimate the temperature of the material at the time point of damage initiation. Best fit to the data suggest that the estimated temperature is  $\approx 600$  K.

Since the temperature of the material can be estimated from the experimental data, the energy balance equation allows estimation of the total energy deposited and, in turn, the fraction of absorbed energy used for heating (to reach the estimated temperature). This estimation suggests that, using a “damage threshold” conduction band electron population density of  $\approx 10^{18}/\text{cm}^3$ , about 50% of the energy absorbed is used for heating while the rest is consumed in other processes (such as shockwave generation, phase transformation, etc.). The model always allows realistic fits using other physically reasonable values of these initial parameters by only modifying the values of  $\Sigma_{i \rightarrow j}$ . This suggests the reliability of the proposed physical scenario and the robustness of the associated model.

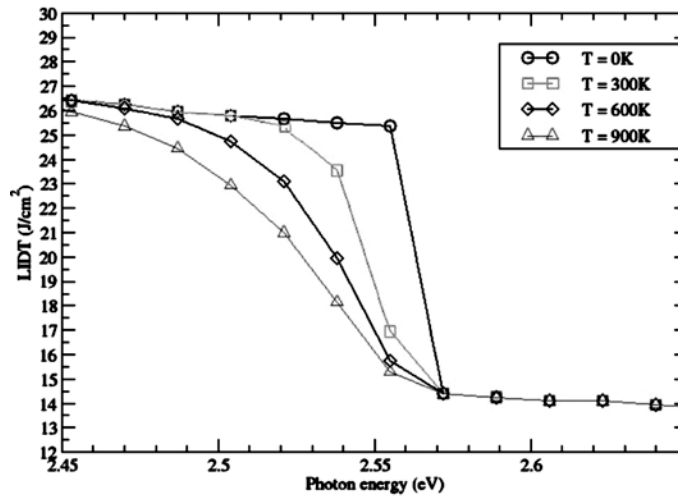


Figure 5. Modeling the “step” of the LIDT vs Temperature highlighting the strong dependence on the temperature.



### 3. DISCUSSION

Our semi empirical approach leads to good agreement between predicted trends and the corresponding experimental observations using a very small number of fitting parameters. The model provides estimates of the excitation and energy balance parameters which have been discussed in detail in Ref. 19. The model suggests a sequence of stages and requirements preceding damage initiation. Specifically, the precursors having a high density of defects and large enough size will initiate damage at lowest fluence. A damage precursor is a cluster of stoichiometric defects with a concentration on the order of  $10^{19}/\text{cm}^3$  and electronic structure that contains distinct excited states. Phase I begins with the heating of the material and secondary defect formation. As the laser intensity remains high for sufficient time (with the time duration of this process depending on the pulse-shape) to heat the material to a certain temperature. When this temperature is reached, quenching of the excited state lifetimes leads to the generation of a quasi-continuum of vibronic states. This represents the onset of phase II. The duration of phase II is on the order of  $\approx 100$  ps, during which the conduction band electron population reaches a density of  $\approx 10^{18}/\text{cm}^3$ . At this point, phase III begins and is associated with a runaway process (of conduction band electron multiplication and plasma formation together with hydrodynamic response of the material [20]) dominating the energy absorption process that is maintained for the remaining length of the pulse. The characteristics of the final damage site depend on the amount of energy deposited during this last phase. Also, the initiation of laser induced damage is associated with the beginning of phase III.

It can be considered that the quasi-continuum of states is not due to the temperature increase but it pre-existed as part of the electronic structure of the defects. This physical model is actually common in ion-doped or color center dielectric material and is manifested by a strong broadband absorption but no emission. The former is due to the quasi-continuum of vibronic states and the latter due to the very short lifetime of the excited states, namely, the relaxation process (following absorption of a photon) is nearly entirely nonradiative. This model can be considered but in order to reproduce the results of Fig. 1b, a wavelength dependent one-photon absorption cross sections ( $\Sigma_{i,j}$ ) must be introduced.

### ACKNOWLEDGEMENTS

This work was performed under the auspices of the U.S. Department of Energy by Lawrence Livermore National Laboratory under Contract DE-AC52-07NA27344. [LLNL-PROC-663105]

### REFERENCES

- [1] C.W. Carr, H.B. Radousky, A.M. Rubenchik, M.D. Feit, S.G. Demos, Phys. Rev. Lett. **92**, 087401-1 (2004)
- [2] A. Salleo, S. T. Taylor, M. C. Martin, W. R. Panero, R. Jeanloz, T. Sands, F. Y. Genin, Nat. Mater. **2**, 796 (2003)
- [3] C. H. Li, X. Jua, J. Huang, X. D. Zhou, Z. Zheng, X. D. Jiang, W. D. Wu, and W. G. Zheng, Nucl. Instrum. Meth. B **269**, 544 (2011)
- [4] M. J. Matthews, C.W. Carr, H. A. Bechtel, and R. N. Raman, Appl. Phys. Lett. **99**, 151109 (2011)
- [5] S.I. Anisimov, B.I. Makshantsev, Sov. Phys. Solid State **15**, 743 (1973)
- [6] N. Bloembergen, Appl. Opt. **12**, 661 (1973)
- [7] C.W. Carr, H.B. Radousky, S.G. Demos, Phys. Rev. Lett. **91**, 127402, 2003
- [8] J. J. Adams, T. L. Weiland, J. R. Stanley, W. D. Sell, R. L. Luthi, J. L. Vickers, C. W. Carr, M. D. Feit, A. M. Rubenchik, M. L. Spaeth, and R. P. Hackel, Proc. SPIE **5647**, 265–278 (2005)
- [9] P. DeMange, C. W. Carr, R. A. Negres, H. B. Radousky, and S. G. Demos, Opt. Lett. **30**, 221-224 (2005)
- [10] P. DeMange, R. A. Negres, A. M. Rubenchik, H. B. Radousky, M. D. Feit and S. G. Demos, Appl. Phys. Lett. **89**, 181922 (2006)
- [11] S. Reyn , G. Duchateau, J. Y. Natoli, L. Lema gn re, Appl. Phys. B **109**, 695-706 (2012)
- [12] S. G. Demos, P. DeMange, R. A. Negres, and M. D. Feit, Opt. Express **18**, 13788-13804 (2010)
- [13] G. Duchateau, M. D. Feit, S. G. Demos, J Appl. Phys. **111**, 093106 (2012)
- [14] S. Papernov, A. W. Schmid, J. Appl. Phys. **92**, 5720 (2002)
- [15] G. A. West and N. S. Clements, J. Lumin. **54**, 245 (1992)
- [16] Z. Y. Zhang, K. T. V. Grattan, A. W. Palmer, V. Fericola, and L. Crovini, Phys. Rev. B **51**, 2656 (1995)
- [17] Z. Zhang, K. T. V. Grattan, and A. Palmer, Phys. Rev. B **48**, 7772 (1993)
- [18] M. Stalder, M. Bass, and B. H. T. Chai, J. Opt. Soc. Am. B **9**, 2271 (1992)
- [19] G. Duchateau, M.D. Feit, S. G. Demos, J Appl. Phys. **115**, 103506 (2012)

[20] G. Duchateau, D. Hébert, L. Hallo, Proc. SPIE **7842**, 78420S (2010)